Studies on the Crystallization Behavior of Nylon-6 in the Presence of Layered Silicates Using Variable Temperature WAXS and FTIR

Smitha S. Nair and C. Ramesh*

Division of Polymer Chemistry, National Chemical Laboratory, Pune 411 008, India

Received June 10, 2004; Revised Manuscript Received November 8, 2004

ABSTRACT: The crystallization of nylon-6 clay nanocomposite was studied by variable temperature wide-angle X-ray scattering (WAXS) and Fourier transform infrared spectroscopy (FTIR). Nylon-6 was found to crystallize into γ phase at 210 °C, as indicated by its characteristic peaks in WAXS. However, an additional peak was observed close but on the lower angle side of the main γ phase peak, indicating the presence of a metastable phase. The extent of metastable phase that developed was dictated by the clay content in the nanocomposite as well as the crystallization conditions. The temperature dependence of the d spacing of the γ phase obtained in the presence of clay layers showed difference from the γ phase obtained by treating nylon-6 in KI/I_2 solution. Variable temperature FTIR studies were conducted on the γ phases for the first time, and it showed definite differences in the spectra of the phases obtained by the two methods.

1. Introduction

Nylon-6 is commercially important and one of the prominent members of the polyamide class of semicrystalline polymers. The structure and morphology of nylon-6 have been extensively investigated. Nylon exhibits polymorphism, and the polymorph depends on the crystallization condition. At room temperature it shows two crystalline modifications, namely the α phase[1] and the γ phase.[2] However, the α phase is unstable at elevated temperatures and transforms into the α′ phase, which is stable until melting.[3,4] On the other hand, the γ phase does not exhibit any crystalline transition on heating and is stable up to melting.[3] The α phase has a monoclinic structure[1] with $a = 0.956$ nm, $b = 1.724$ nm, $c = 0.801$ nm, and $\beta = 67.5°$. In the α phase, the hydrogen bonds are formed between antiparallel chains.[1] The γ phase also has a monoclinic structure with $a = 0.933$ nm, $b = 1.688$ nm, $c = 0.478$ nm, and $\beta = 121°$, but the twisted chains allow hydrogen bonds to be formed between parallel chains.[2] The α phase is easily obtained by melt crystallization, while severe crystallization conditions need to be applied to obtain the γ phase. The α phase can be transformed into the γ phase by treatment with aqueous potassium iodide−iodine solution.[2,5−7] High-speed spinning also yields the γ phase.[7] In the case of nylon-6 fibers a metastable phase has also been reported and discussed in detail.[7]

Recently, it has been found that the γ phase is readily formed in nylon-6 nanocomposites, primarily the nylon-6−montmorillonite clay nanocomposites.[8−11] The relative fraction of α and γ phases is dependent on the layered silicate content as well as the interaction between nylon-6 and the silicate layers.[12] It has been shown that the silicate layers act as nucleating centers, and the interaction between the clay layers and the polymer changes its semicrystalline morphology.[13] It has been suggested that the clay surface induces kinetically favored formation of γ phase.[14] Wu and co-workers[15,16] have shown that higher cooling rates promote the crystallization of γ phase. They also reported higher amounts of γ phase when annealed at 200 °C as against 180 °C. Paul et al.[17] studied the crystallization behavior of nylon-6−clay nanocomposites and observed that in the case of injection-molded samples the γ phase predominates in the skin while the core contains both forms, which is attributed to the different cooling rates of the skin and core regions.

Variable temperature WAXS is perhaps the most appropriate tool to study the crystalline phases and their transitions. The crystallization of nylon-6−clay nanocomposite from the melt has been monitored by using a hot stage coupled to an X-ray diffractometer. We have observed for the first time the appearance of the metastable phase, apart from the γ phase, during the crystallization of nylon-6 in the presence of silicate layers. Further, for the first time, we report the examination of the γ phase of nylon-6 in the nanocomposite and the γ phase obtained by treating nylon-6 in KI/I_2 by variable temperature FTIR spectroscopy.

2. Experimental Section

Nylon-6 pellets (Akulon K2 2D grade, IV = 0.76 dL/g) were obtained from Century Enka, India. The clays, Cloisite 25A (MMT-C_8H_{17}) and Cloisite 30B (MMT- $(CH_2CH_2OH)_2$), were obtained from Southern Clay Products. These clays were montmorillonites modified by dimethyl 2-ethylhexyl (hydrogenated tallow alkyl) ammoniums and methyl bis(2-hydroxyethyl) (hydrogenated tallow alkyl) ammoniums, respectively. Before melt mixing, nylon-6 and the clays were dried in a vacuum oven at 100 °C for 5 h. In most cases, melt mixing (100 rpm) of nylon-6 with the desired amount of clay was conducted in a DSM Micro 5 twin screw compounder at 230 °C for 5 min. The batch size was approximately 5 g. In one case the mixing was performed in Haake Rheocord 600p attached with a batch mixer (75 rpm, 230 °C for 5 min), and the batch size was approximately 50 g. The strands obtained were powdered in a SPEX 6750 freezer mill. The TGA-7 unit in the Perkin-Elmer thermal analysis system was used to determine the amount of clay present in the nanocomposites. The samples were heated under a flowing nitrogen atmosphere from 50 to 600 °C, at a heating rate of 10 °C/min, and the weight loss was recorded. The weight of the residue remaining at 600 °C was taken as the % clay content in the nanocomposite. The X-ray diffraction experiments were performed using a Rigaku Dmax 2500 diffractometer with a copper target. The details are described elsewhere.[3] The following slits were used to maximize the resolution: divergence slit, 0.5°; scattering slit, 0.5°; receiving slit, 0.15 mm.

10.1021/ma048860d CCC: $30.25
Published on Web 12/30/2004

The low cooling rate of the hot stage made it impossible to in situ crystallize below 200 °C because the sample crystallized prior to reaching the intended crystallization temperature. Hence, a different method was followed for crystallization at lower temperatures. Powders of the nylon/clay nanocomposites were sandwiched between two thin microscopic cover glasses, heated on a hot plate, melted, and pressed into a thin film. The sandwiched films were melted for about 5 min in an oil bath isothermally set at 240 °C and then very rapidly transferred to another oil bath maintained at the crystallization temperature. After crystallization in the oil bath, the sample was recovered and transferred to the X-ray hot stage, and the change in structure was monitored during heating by scanning at regular temperature intervals. The crystallinity of the samples was calculated from the integrated intensity of the crystalline reflections and the amorphous scattering.

Room-temperature and high-temperature infrared spectra of these samples were taken using a Perkin-Elmer FTIR spectrometer (model: Spectrum GX) with a DTGS detector at a resolution of 2 cm^{-1} in the range of 400−4500 cm^{-1}. A total of 32 scans were used for signal averaging. The high-temperature spectra were obtained by mounting the sample in the Mettler Toledo FP82HT hot stage and placing it in the sample compartment of the FTIR. The sample, in the form of powder, was sandwiched in the KBr pellet. The sample was heated at a rate of 10 °C/min. The spectra were collected while the sample temperature was held constant. The change in spectra was monitored during heating by scanning at regular temperature intervals until the sample melted. The selected regions of the spectra were deconvoluted using Peakfit (Jandell) deconvolution program, and the profiles were assumed to be Gaussian. Nylon-6 in the α phase was obtained by dissolving nylon-6 in 1,4-butanediol at its refluxing temperature and subsequently cooling very gradually to room temperature. This procedure gave highly crystalline α phase in the form of fine powder. This powder was used for FTIR studies on the α phase as well as to obtain the γ phase, as described elsewhere.[3] In the case of nylon-6−clay sample, the γ phase was obtained by the following method: A very thin film of the nylon-6−clay sample was melt-pressed in a small copper plate and allowed to cool to room temperature. The room-temperature WAXS pattern showed that the sample crystallized fully into γ phase, and the crystallinity was 37%.

3. Results and Discussion

3.1. Variable Temperature WAXS Studies. The nanocomposites obtained are either intercalated or exfoliated depending on the type of clay used. The gallery height of Cloisite 25A and Cloisite 30B, as determined from the X-ray diffraction experiments, are 1.84 and 1.78 nm, respectively. Cloisite 25A yields always intercalated nanocomposites as evident from the characteristic clay layer peak at $2\theta = 2.48°$ and 5.22°. On the other hand, Cloisite 30B-based nanocomposites appear to be exfoliated, as the characteristic clay peaks are absent in the X-ray diffractograms. The exfoliation in the case of Cloisite 30B is probably due to the presence of high hydroxyl content in the clay surface compared to Cloisite 25A. However, under the experimental conditions used, the crystallization behavior of nylon-6 is similar for both the nanocomposites. Hence, the crystallization data obtained from the intercalated system is presented here because additional information is available on the effect of nylon crystallization on the clay layers.

The structure development during isothermal crystallization of nylon-6−clay nanocomposite at 210 °C and subsequent cooling to room temperature has been followed in-situ by WAXS. The behavior of the diffractograms and the d spacing on cooling from the crystallization temperature (T_c) to room temperature are shown in parts a and b of Figure 1, respectively. The clay peaks observed at low 2θ ranges are not shown in the figure but will be discussed separately. The salient feature of Figure 1a is that the diffractogram recorded after the completion of crystallization at 210 °C shows two sharp peaks at $2\theta = 20.33°$ and 20.93°, and the corresponding d spacings are 0.437 and 0.424 nm, respectively. A third peak appears as a shoulder to the peak at $2\theta = 20.93°$ and is at $2\theta = 21.54°$. The peaks at $2\theta = 20.93°$ and 21.54 ° may be identified as 100 and 200/$\bar{2}$01 reflections of the γ phase. The peak at $2\theta = 20.33°$ is observed for the first time and is indicative of the presence of an additional phase as this peak is not observed for the γ phase. The position of this new reflection is closer to the 200 reflection of the α phase. Nevertheless, its behavior on cooling differs from the α phase[3,4] and will be discussed in the following paragraph. Following Murthy,[7] the second phase may be interpreted to arise from the 200 reflection of an intermediate phase and is termed the metastable phase to distinguish it from the α and γ phases. Murthy[7] showed that the metastable phase can be converted into either the α or γ phase by suitable thermomechanical treatment. The deconvolution procedure could not locate the 002/202 peak of the metastable phase, and hence it is not considered during the deconvolution process.

The characteristic peaks of the γ phase at $2\theta = 20.93°$ and 21.54° show a small shift toward higher angles due to thermal contraction on cooling to room temperature.

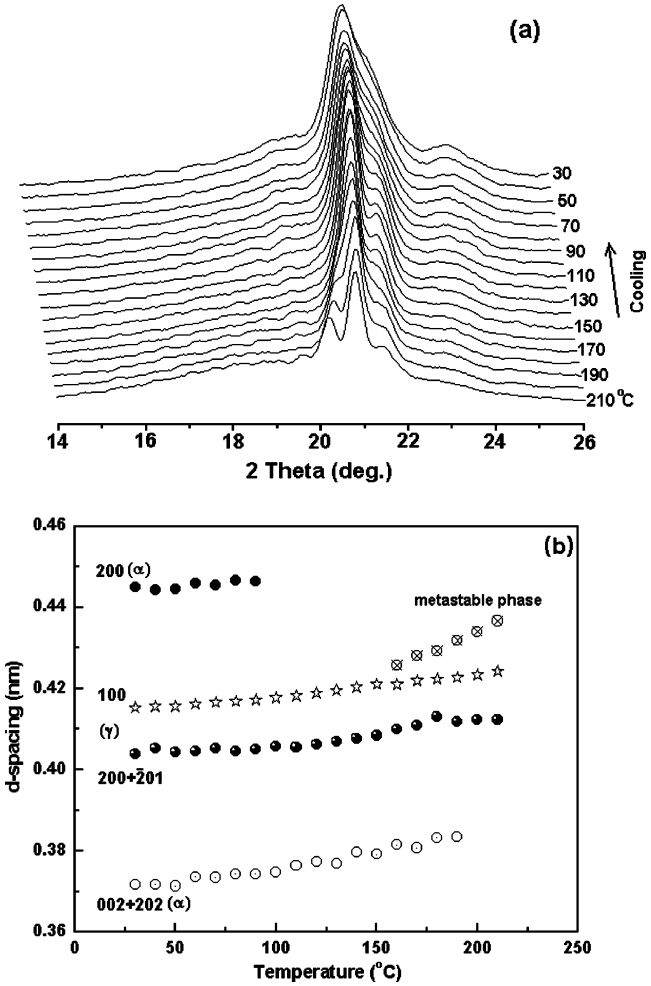

Figure 1. (a) Behavior of X-ray diffraction patterns and (b) d spacings on cooling from T_c to room temperature of nylon-6 cloisite 25A nanocomposite (6%).

On the other hand, the response of the metastable phase on cooling is more dramatic; the peak at $2\theta = 20.33°$ shifts toward higher values and merges with the 100 reflection of the γ phase at around 150 °C. Below 150 °C the metastable phase could not be distinguished from the γ phase. This may be due to an anisotropic thermal contraction of the lattice planes corresponding to these two X-ray peaks. Though the crystallization of nylon-6 in the presence of clay is predominantly in the γ phase, the α phase is also formed to some extent. The trace of the α phase is first seen at 190 °C, as the 002/202 reflection of the α phase is seen distinctly at this temperature. On the other hand, the 200 reflection becomes apparent only after cooling below 100 °C. The d spacings of the α phase reflections are shown in Figure 1b along with that of the γ phase. At room temperature the amount of the γ phase is 40% and that of the α phase is 9%. The variations in diffraction patterns and d spacings on cooling from T_c are found to be reversible on heating and hence will not be discussed in detail. The behavior of the γ phase obtained in the presence of silicate layers may be compared with the γ phase obtained by treating nylon-6 in KI/I_2 solution. In the latter case, no metastable phase is observed at 160 °C on heating but remained as the γ phase until melting.[3]

It is worth comparing the d spacing of the γ phases crystallized in the presence of clay layers with that of the γ phase observed in neat nylon. The characteristic d spacings of the 100 and 200/$\bar{2}$01 reflections of the γ phase of neat nylon-6 obtained by KI/I_2 treatment at room temperature are 0.415 and 0.40 nm, respectively.[3] These values do not change appreciably at 210 °C and are 0.419 and 0.404 nm. In the case of γ phase obtained in the presence of clay layers the d spacings are similar at room temperature. However, these values change to 0.424 and 0.412 nm at 210 °C, indicating the existence of a definite difference between the γ phases obtained by the two methods.

A careful observation of the diffractograms in Figure 1a shows the continued crystallization of the material in the γ phase during cooling to room temperature. Simultaneously, there is an increase in the fraction of the α phase during cooling, albeit in low fractions. The crystallization of nylon-6 into the γ phase is assisted by the clay layers, and this is evident from the crystal size calculated from the reflections 100 and 200/$\bar{2}$01. The crystal size, 28 nm, normal to the plane 100 is unusually large and shows that the clay layer acts as a template for epitaxial crystallization[18] of nylon-6. The large crystal size indicates that at 210 °C most of the crystallization occurs close to clay layers; but on cooling, crystallization could take place farther removed from the clay layers with reduced crystal sizes, thereby broadening the diffraction peaks. The amount of α phase fraction formed depends on the crystallization condition. The thin film sample allowed to crystallize on cooling to ambient temperature showed only the γ phase without any α phase at room temperature.

The X-ray diffraction patterns of the sample crystallized in the silicon oil bath at 100 °C are shown in Figure 2. At room temperature the sample exhibits a typical γ phase along with a small amount of α phase, which is consistent with the observations of Fornes and Paul.[17] On heating, the α phase disappears at a lower temperature than the sample crystallized at 210 °C. The metastable phase appears at about 160 °C and coexists with γ phase until melting. These results further

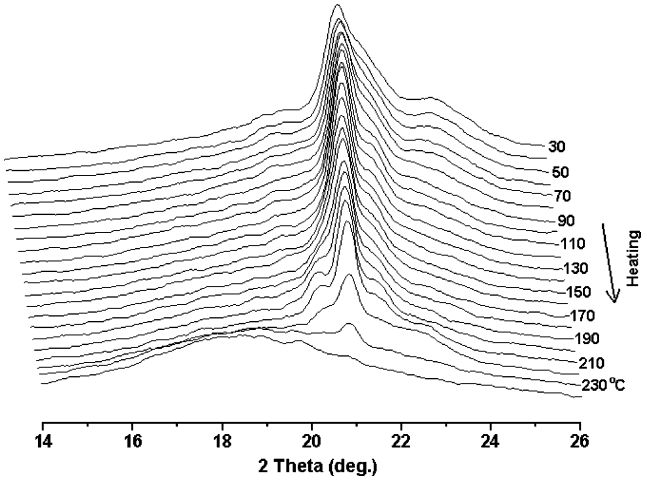

Figure 2. Behavior of X-ray diffraction patterns on heating from room temperature to melt of nylon-6 cloisite 25A nanocomposite (5.5%) crystallized in a silicone oil bath at 100 °C (sample prepared in Haake Rheocord).

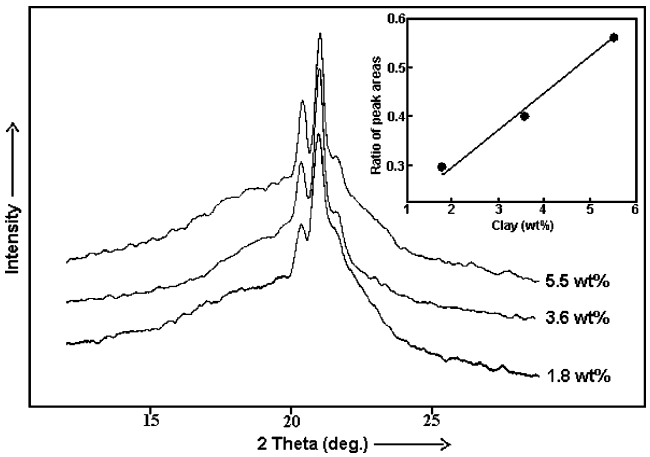

Figure 3. X-ray diffraction patterns at the end of crystallization at 210 °C for various clay contents of nylon-6 clay nanocomposites. Inset shows the ratio of the 200 peaks of the metastable and γ phases at 210 °C.

indicate that the metastable phase also crystallized along with γ phase at 100 °C but could not be distinguished from the γ phase because the d spacings overlap in the temperature range from room temperature to 150 °C. However, the intensity of the 200 reflection of the metastable phase is lower than the intensity of the sample crystallized at 210 °C, indicating that the crystallization temperature is one of the factors that control the formation of the metastable phase. The amount of metastable phase crystallized also appears to depend on the clay content in the nanocomposite. The diffractograms recorded at the end of crystallization at 210 °C for various clay contents are shown in Figure 3. It may be commented that the amount of metastable phase depends on the amount of clay present in the nanocomposite and the crystallization temperature. At this stage it may be speculated that the metastable phase is the material directly crystallizing on the clay layers and can be seen only after heating above 150 °C. The metastable phase is shown to transform into the α or γ phase by suitable thermomechanical treatment;[7] apparently, in the present case the metastable phase is formed and stabilized by the clay layers.

The effect of crystallization of nylon-6 on the clay layers in the case of intercalated nanocomposites will

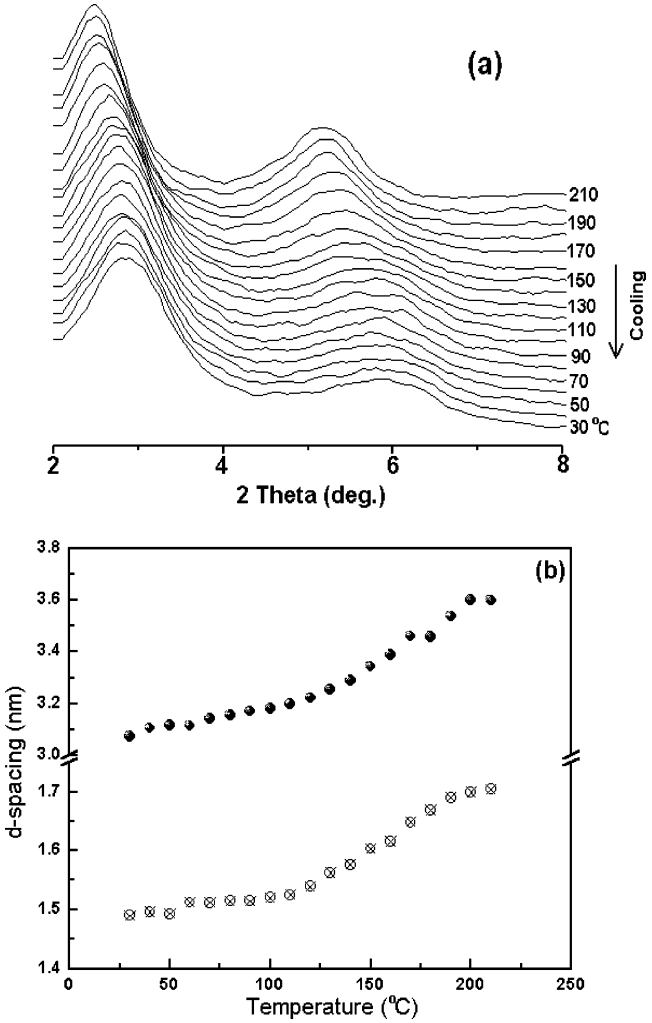

Figure 4. Behavior of (a) X-ray diffraction patterns and (b) d spacings of clay at low 2θ ranges on cooling from T_c (210 °C) to room temperature for nylon-6 cloisite 25A nanocomposite (6%).

be discussed here. Figure 4a shows the variation of diffraction patterns at low 2θ ranges, where characteristic peaks due to clay occur, during cooling from the crystallization temperature. The clay exhibits two peaks at $2\theta = 2.48°$ and 5.22°, corresponding to d spacings of 3.59 and 1.70 nm at the crystallization temperature, 210 °C. These are the first- and second-order reflections from the clay layers.[19] The d spacing 3.59 nm corresponds to the distance between two adjacent clay layers and is called the gallery height. Figure 4b shows the variation of gallery height with temperature on cooling. The gallery height decreases with decreasing temperature; however, it decreases more rapidly on cooling from 190 to 130 °C and may be attributed to the crystallization of nylon-6 present within the gallery. At 210 °C the crystallization rate of nylon-6 within the gallery will be retarded due to the confined space, and it is kinetically favored to crystallize at lower temperatures on cooling. Apart from the changes in gallery height, the clay peaks become broader and decrease in peak height. These changes suggest some degree of disturbance in the clay layer stacking order due to polymer crystallization within the layers. However, these changes are reversible on heating as the material crystallized between the clay layers melts away.

3.2. Variable Temperature FTIR Studies. The foregoing discussions are primarily focused on the structure based on the data obtained from variable temperature WAXS studies, and in the following section the discussion will be focused on the data obtained from variable temperature FTIR studies on the γ phase of nylon-6 in the presence and absence of clay layers. Variable temperature spectra of the α phase are also obtained and compared with the spectra of γ phase. It may be pointed out that Murthy and co-workers[20] obtained the α phase by melt crystallization while in the present case the α phase is obtained by dissolving nylon-6 in 1,4-butanediol at its refluxing temperature and subsequent slow cooling to room temperature. The crystallinity of the sample at room temperature is 56%; the infrared spectra obtained at room temperature and on heating look similar to the variable temperature spectra reported by Murthy and co-workers,[20] and hence it will not be discussed here. It is interesting to note that when the α phase, with 56% crystallinity, is converted into the γ phase (KI/I_2) by treating in KI/I_2 solution at room temperature, the crystallinity decreases to 36%. The room-temperature WAXS indicates the absence of the α phase in the sample. The large decrease in the crystallinity during phase transformation indicates the occurrence of major structural reorganization when the α phase converts into the γ phase. Variable temperature WAXS studies on these samples are reported in detail elsewhere,[3] and here we report for the first time the variable temperature FTIR spectra of the γ phase obtained by treating nylon-6 in KI/I_2 solution and the γ phase (clay) obtained by melt crystallization of nylon-6 clay nanocomposite.

The infrared spectroscopy studies on nylon-6 have been made, and the band assignments of α and γ phases are reported in the literature.[21−28] The γ phase (KI/I_2) shows distinct absorbance peaks at 585, 623, 962, 975, 1234, and 1439 cm^{-1}. On the other hand, the α phase shows strong characteristic bands at 577, 928, 950, 959, 1201, 1416, and 1477 cm^{-1}. The γ phase (clay) shows absorbance bands at 588, 626, 962, 974, 1235, and 1439 cm^{-1}. The 463, 1020, and 3628 cm^{-1} bands are due to clay and are obvious only in the nylon-6−clay spectra. Figures 5−8 show the sections of spectra of α and γ phases wherein major differences are observed between the phases.

Figure 5a−c shows the spectral region from 400 to 800 cm^{-1} for the various phases and comprises amide V and amide VI bands. At room temperature the amide V and VI bands appear at 690 and 577 cm^{-1}, respectively, for the α phase. The amide V band shifts to 710 cm^{-1} for the γ phase (KI/I_2). The amide VI band is shifted[28] to 623 cm^{-1} from 577 cm^{-1}. However, in Figure 5b the spectra show a distinct additional band at 585 cm^{-1} and may be assigned exclusively to the γ phase (KI/I_2) because the α phase is totally absent in this sample, as evidenced from the WAXS pattern at room temperature. This may also be assigned to the amide VI band because of the position, and hence in the case of the γ phase amide VI has two distinct bands at 585 and 623 cm^{-1}. The spectra of the γ phase (clay), as seen from Figure 5c, are very similar to the spectra of the γ phase (KI/I_2), but with band shifts for the key amide bands. The amide V appears at 713 cm^{-1} while the two bands of amide VI occur at 588 and 626 cm^{-1}. The variation of amide V band position on heating for α and γ phases is shown in Figure 5d. On heating, the wavenumber of amide V band decreases with increasing temperature; the decrease is more for the γ phase than

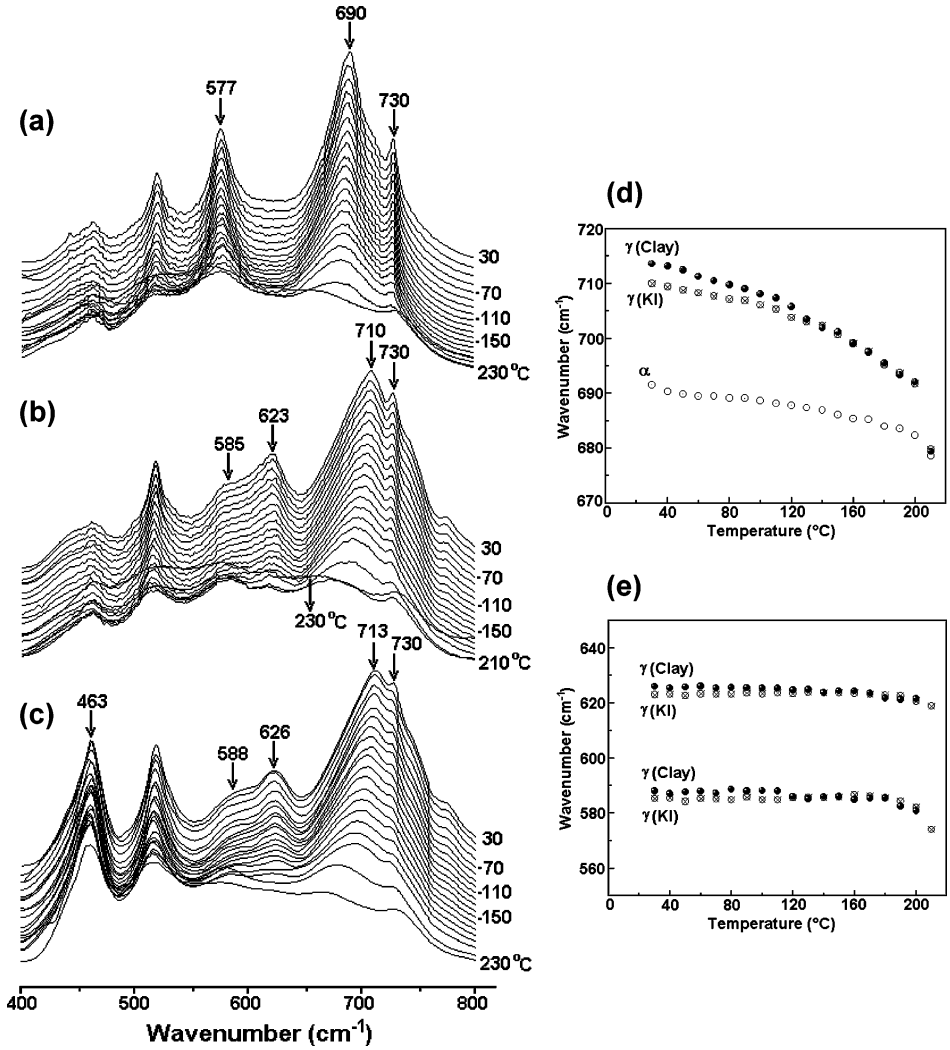

Figure 5. Variable temperature FTIR spectra of the region 400−800 cm^{-1} of nylon-6 during heating from room temperature to melt: (a) α phase; (b) γ phase obtained by treating the α phase in KI/I_2 solution at room temperature; (c) γ phase obtained by melt crystallization of nylon-6-clay nanocomposite; (d) variation of the wavenumber of amide V band at 690 cm^{-1} for all the three phases during heating; (e) variation of the wavenumber of amide VI band at 577 cm^{-1} for all the three phases and the amide VI band at 623 cm^{-1} for the γ phases during heating.

the α phase. Both the γ phases have same wavenumber above 120 °C, and interestingly in the melt above 210 °C the phases vanish and all the samples show the same wavenumber, 678 cm^{-1}. The amide VI bands at 585 and the 623 cm^{-1} show very small decrease with increase in temperature. Again, above 120 °C the γ phase (clay) and the γ phase (KI/I_2) have the same wavenumber. On heating close to melting temperature, the wavenumber shows a more rapid downward shift, and these bands vanish in the melt. Another interesting feature is the band at 730 cm^{-1} assigned to the methylene rocking mode, which arises from the orthorhombic packing cell of the methylene segments.[29−31] The band at 730 cm^{-1} appears for all the three samples at the same wavenumber, indicating that the conformation of the methylene segments is similar for the α and γ phases, even though the hydrogen-bonding schemes are different. The 730 cm^{-1} band disappears when the sample melts at 210 °C. The band at 463 cm^{-1} is due to the clay and does not change even at 230 °C, while the nylon-6 is in the melt form at this temperature.

Figure 6 shows the spectra in the region from 900 to 1050 cm^{-1}. The α phase shows characteristic absorbance peaks at 928, 950, and 959 cm^{-1}. These bands do not appear for the γ phases, but new bands appear at 962 and 975 cm^{-1}. The band at 975 cm^{-1} is assigned to the CO−NH in-plane vibration.[23,26] The band appears at 974 cm^{-1} at room temperature for the γ phase (clay). On heating, the 975 cm^{-1} band of the γ phase (KI/I_2) shows a small shift to lower wavenumber, but the band at 974 cm^{-1} exhibits a shift toward the higher wavenumber. The band at 962 cm^{-1} appears to vanish well below the melting temperature; however, the deconvolution of the peaks indicates that the 962 cm^{-1} band exists up to the melting temperature, albeit, with greatly reduced intensity. The peak width increases with increase in temperature, but the normalized absorbance decreases. The γ phase (KI/I_2) and the γ phase obtained in the presence of clay show similar behavior in the half-width and the normalized absorbance, but minor variations can be seen. In the case of nylon clay nanocomposites the band at 1050 cm^{-1} is due to Si−O stretch of the clay layers.[32]

Another region of interest is from 1150 to 1300 cm^{-1}, and the γ phase shows a distinct characteristic absorbance at 1234 cm^{-1}, which is assigned to amide III and CH_2 wagging vibration.[22,26] Figure 7a−f shows the spectra in this region and the behavior of the wavenumber, peak half-width, and the normalized intensity of the characteristic γ phase band. The band appears

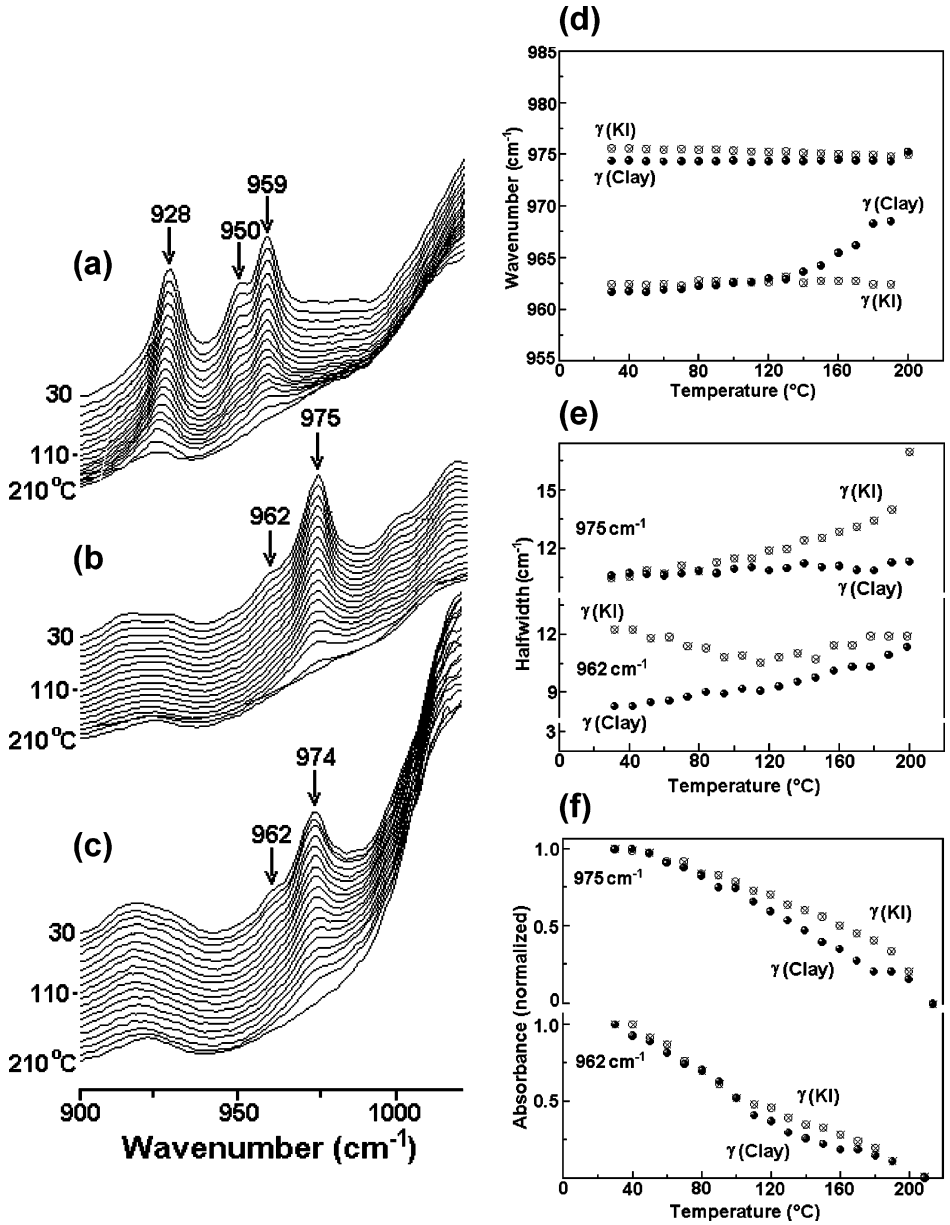

Figure 6. Variable temperature FTIR spectra of the region 900−1050 cm^{-1} of nylon-6 during heating from room temperature to melt: (a) α phase; (b) γ phase obtained by treating α phase in KI/I_2 solution at room temperature; (c) γ phase obtained by melt crystallization of nylon-6−clay nanocomposite. The variation of (d) wavenumber, (e) full width at half-maximum, and (f) normalized absorbance for the 962 and 975 cm^{-1} bands for the γ phases during heating.

at 1234 and 1235 cm^{-1} for the γ phase (KI/I_2) and γ phase (clay), respectively. On heating, the wavenumbers show marginal decrease up to 180 °C. On heating above 180 °C, in the case of the γ phase (clay) the wavenumber shifts to lower value, but it increases in the case of the γ phase (KI/I_2). The half-width increases with increase in temperature, and above 150 °C the half-width shows more accelerated increase. However, the normalized absorbance decreases with increase in temperature. The key difference between the γ phase obtained by KI/I_2 treatment and the γ phase (clay) is the half-width of the band. The γ phase (clay) shows consistently higher half-width compared with the γ phase obtained by KI/I_2 treatment.

The region from 3100 to 3500 cm^{-1} is very sensitive to hydrogen bonding and is assigned to the hydrogen-bonded NH stretch (amide A). The contribution to the amide A comes from (i) free N−H stretch at 3444 cm^{-1}, (ii) bonded N−H stretch at 3300 cm^{-1} arising out of crystalline fraction, and (iii) bonded N−H stretch at 3310 cm^{-1} arising out of amorphous fraction. The region is too broad to deconvolute meaningfully into individual peaks and hence is discussed as a composite peak. Nevertheless, it provides valuable information, and Figure 8 shows the variable temperature spectra of the α and γ phases along with the wavenumber variation with temperature for the band at 3300 cm^{-1}. Qualitatively, the spectra of the γ phases look similar, but the peak occurs at 3301 and 3305 cm^{-1} for the γ phases obtained by KI/I_2 and clay, respectively. Another observable difference is that in the case of γ phase (clay) the band appears broader than the γ phase (KI/I_2). The amide A band appears at 3301 cm^{-1} for the α phase, and the band is sharper than the γ phases. On heating, the band shifts to higher wavenumber region, and all the samples have similar shape and wavenumber in the melt above 210 °C. The bands at 2868 and 2940 cm^{-1} need special mention; these bands are not related to

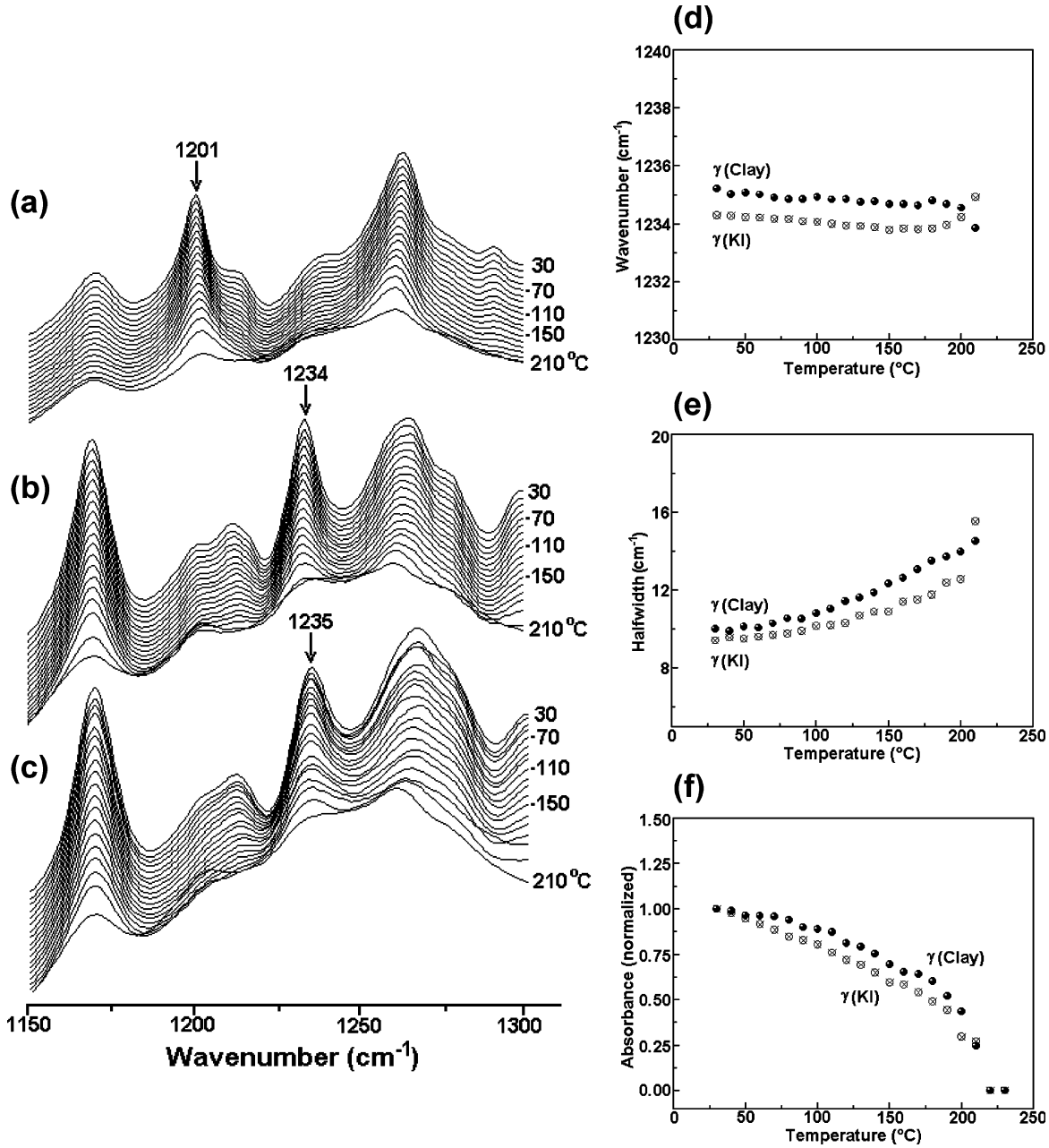

Figure 7. Variable temperature FTIR spectra of the region 1150−1300 cm^{-1} of nylon-6 during heating from room temperature to melt: (a) α phase; (b) γ phase obtained by treating α phase in KI/I_2 solution at room temperature; (c) γ phase obtained by melt crystallization of nylon-6-clay nanocomposite. The variation of (d) wavenumber, (e) full width at half-maximum, and (f) normalized absorbance for the 1234 cm^{-1} band for the γ phases during heating.

crystalline fraction because these bands are present without much reduction in absorbance above the melting temperature. These bands are assigned to symmetric and asymmetric CH_2 stretch, respectively.[21,25] The nature of the crystalline phase seems to affect the peak position of these bands. At room temperature these bands appear at 2869 and 2940 cm^{-1} for the α phase. These bands shift to 2858 and 2929 cm^{-1} for the γ phase (KI/I_2) and to 2860 and 2933 cm^{-1} for the γ phase (clay). Interestingly, the values converge to 2860 and 2934 cm^{-1} in the melt for all the samples. The effect of interaction between the nylon and clay is also seen in the spectra of clay as well. The band due to hydrogen bonding is seen at 3633 cm^{-1} for the modified clay at room temperature. This band shifts to 3628 cm^{-1} for the nylon-6-clay nanocomposite; shifting of the wavenumber toward lower frequency indicates the strengthening of the hydrogen bonding in the clay due to nylon-6.

The samples used for FTIR studies have only one phase present at room temperature, and the FTIR spectra may be considered to represent the respective phases. Further, the crystallinity of the samples having the γ phase is similar and is about 36%. The variable temperature FTIR spectra of the γ phase (clay) do not indicate the presence of metastable phase, even though WAXS studies showed its presence. The possible argument is that the chain conformation in the metastable phase is similar to the γ phase and hence could not be identified in the FTIR spectra. The difference seen in the FTIR spectra of the γ phases is similar to the differences exhibited by the samples in the behavior of d spacing, even though the general feature of the γ phase is similar in both the samples. The difference may

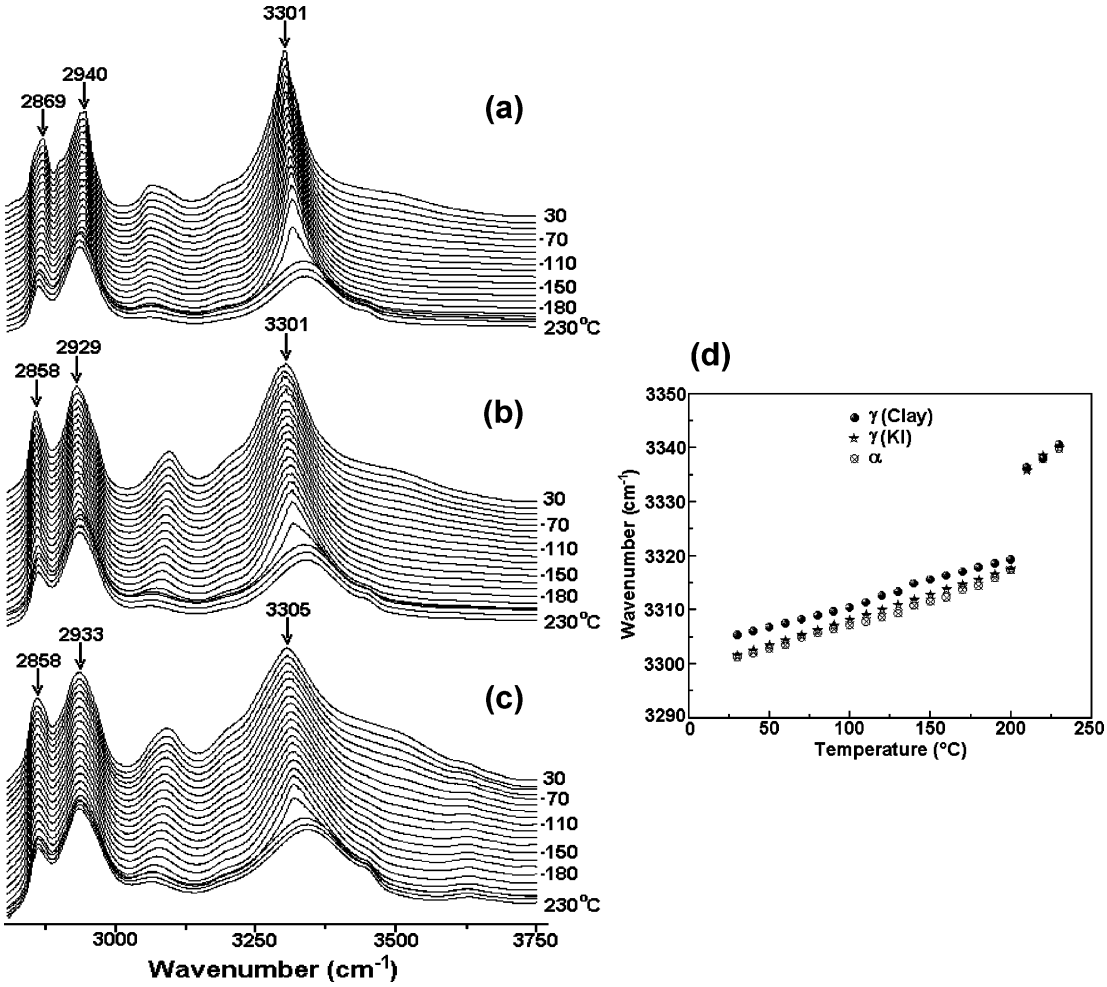

Figure 8. Variable temperature FTIR spectra of the region 2750−3750 cm^{-1} of nylon-6 during heating from room temperature to melt: (a) α phase; (b) γ phase obtained by treating α phase in KI/I_2 solution at room temperature; (c) γ phase obtained by melt crystallization of nylon-6−clay nanocomposite; (d) variation of the wavenumber of amide A band at 3301 cm^{-1} with temperature for all three samples.

be attributed to the mechanism of γ phase formation, which is different for the two methods. In the case of the nanocomposite, the γ phase is formed by melt crystallization with clay layers controlling the hydrogen bonds. In the case of the γ phase obtained by KI/I_2 treatment, the iodine forms a complex with the nylon, and the removal of iodine from the complex leads to the γ phase.[28]

4. Conclusion

The in situ X-ray diffraction studies on the crystallization of nylon-6−clay nanocomposites provided new information on the crystallization of nylon-6 in the presence of clay layers. Nylon-6 in the nanocomposite is crystallized into the γ phase and metastable phase. The metastable phase depended on the amount of clay present in the system and is obvious in the X-ray diffractogram only after heating to 150 °C. The d spacings of the nylon-6 γ phase obtained in the presence of the clay showed differences from the pristine γ phase obtained by treating nylon-6 in KI/I_2 solution. The variable temperature FTIR spectroscopy studies also showed that the nylon clay system gives characteristic infrared bands at different positions from those of the neat γ phase. These results suggest that in the case of nylon-6 the characteristics of the γ phase depend on the method of its formation.

Acknowledgment. The authors thank Dr. S. Sivaram, Director, National Chemical Laboratory, for his keen interest and encouragement during the course of this work. S.S.N. acknowledges the Council of Scientific and Industrial Research, New Delhi, for the award of a research fellowship.

References and Notes

(1) Holmes, D. R.; Bunn, C. W.; Smith, D. J. *J. Polym. Sci.* **1955**, *17*, 159.
(2) Arimoto, H.; Ishibashi, M.; Hirai, M.; Chatani, Y. *J. Polym. Sci., Part A* **1965**, *3*, 317.
(3) Ramesh, C.; Gowd, E. B. *Macromolecules* **2001**, *34*, 3308.
(4) Murthy, N. S.; Curran, S. A.; Aharoni, S. M.; Minor, H. *Macromolecules* **1991**, *24*, 3215.
(5) Stepaniak, R. F.; Garton, A.; Carlsson, D. J.; Wiles, D. M. *J. Polym. Sci., Polym. Phys. Ed.* **1979**, *17*, 987.
(6) Miyasaka, K.; Makishima, K. *J. Polym. Sci., Part A-1* **1967**, *5*, 3017.
(7) Murthy, N. S. *Polym. Commun.* **1991**, *32*, 301.
(8) Kojima, Y.; Usuki, A.; Kawasumi, M.; Okada, O.; Fukushima, Y.; Kurachi, T.; Kamigaito, O. *J. Mater. Res.* **1993**, *8*, 1185.
(9) VanderHart, D. L.; Asano, A.; Gilman, J. W. *Chem. Mater.* **2001**, *13*, 3781.
(10) Lincoln, D. M.; Vaia, R. A.; Wang, Z. G.; Hsiao, B. S. *Polymer* **2001**, *42*, 1621.
(11) Cho, J. W.; Paul, D. R. *Polymer* **2001**, *42*, 1083.
(12) Lincoln, D. M.; Vaia, R. A.; Wang, Z. G.; Hsiao, B. S.; Krishnamoorti, R. *Polymer* **2001**, *42*, 9975.
(13) Lincoln, D. M.; Vaia, R. A.; Krishnamoorti, R. *Macromolecules* **2004**, *37*, 4554.

(14) Mathias, L. J.; Davis, R. D.; Jarrett, W. L. *Macromolecules* **1999**, *32*, 7958.
(15) Wu, Q.; Liu, X.; Berglund, L. A. *Macromol. Rapid Commun.* **2001**, *22*, 1438.
(16) Liu, X.; Wu, Q. *Eur. Polym. J.* **2002**, *38*, 1383.
(17) Fornes, T. D.; Paul, D. R. *Polymer* **2003**, *44*, 3945.
(18) Maiti, P.; Okamoto, M. *Macromol. Mater. Eng.* **2003**, *288*, 440.
(19) Vaia, R. A.; Ishii, H.; Giannelis, E. P. *Chem. Mater.* **1993**, *5*, 1694.
(20) Vasanthan, N.; Murthy, N. S.; Bray, R. G. *Macromolecules* **1998**, *31*, 8433.
(21) Doskocilova, D.; Pivcova, H.; Schneider, B.; Cefelin, P. *Collect. Czech. Commun.* **1963**, *28*, 1867.
(22) Schneider, B.; Schmidt, P.; Wichterle, O. *Collect. Czech. Commun.* **1962**, *27*, 1749.
(23) Illers, K. H.; Haberkorn, H.; Simak, P. *Makromol. Chem.* **1972**, *158*, 285.
(24) Jakes, J.; Krimm. S. *Spectrochim. Acta* **1971**, *27A*, 19.
(25) Jakes, J.; Krimm. S. *Spectrochim. Acta* **1971**, *27A*, 35.
(26) Rotter, G.; Ishida, H. *J. Polym. Sci., Polym. Phys. Ed.* **1992**, *30,* 489.
(27) Wu. Q.; Liu. X.; Berglund, L. A. *Polymer* **2002**, *43*, 2445.
(28) Abu-isa, I. *J. Polym. Sci., Part A-1* **1971**, *9*, 199.
(29) Snyder, R. G. *J. Chem. Phys.* **1979**, *71*, 3229.
(30) Tashiro, K.; Sasaki, S.; Kobayashi, M. *Macromolecules* **1996**, *29*, 7460.
(31) Yoshioka, Y.; Tashiro, K.; Ramesh, C. *Polymer* **2003**, *44*, 6407.
(32) Loo, L. S.; Gleason, K. K. *Macromolecules* **2003**, *36*, 2587.

MA048860D